Primary Electron Transfer in Membrane-Bound Reaction Centers with Mutations at the M210 Position

ARTICLE *in* THE JOURNAL OF PHYSICAL CHEMISTRY · APRIL 1996

Impact Factor: 2.78 · DOI: 10.1021/jp953054h

Primary Electron Transfer in Membrane-Bound Reaction Centers with Mutations at the M210 Position

L. M. P. Beekman,*,† I. H. M. van Stokkum,† R. Monshouwer,† A. J. Rijnders,† P. McGlynn,‡ R. W. Visschers,§ M. R. Jones,‡ and R. van Grondelle†

Department of Physics and Astronomy and Department of Plant Physiology, Vrije Universiteit, De Boelelaan 1081, 1081 HV, Amsterdam, The Netherlands, and Krebs Institute for Biomolecular Research and Robert Hill Institute for Photosynthesis, Department of Molecular Biology and Biotechnology, University of Sheffield, Western Bank, Sheffield S10 2UH, United Kingdom

Received: October 16, 1995; In Final Form: January 9, 1996[⊗]

The kinetics of primary electron transfer in membrane-bound *Rhodobacter sphaeroides* reaction centers (RCs) were measured on both wild-type (WT) and site-directed mutant RC's bearing mutations at the tyrosine M210 position. The tyrosine was replaced by histidine (H), phenylalanine (F), leucine (L), or tryptophan (W). A mutant with histidine at both the M210 and symmetry-related L181 positions (YM210H/FL181H) was also examined. Rates of primary charge separation were determined by both single and multiple wavelength pump−probe techniques. The time constants for the decay of stimulated emission in the membrane-bound mutant RC's were approximately 27 ps (F), 36 ps (L), 72 ps (W), 5.8 ps (H), and 4.2 ps (HH), compared with 4.6 ps in WT membrane-bound RC's. For all RC's, the decay of stimulated emission was found to be multiexponential, demonstrating that this phenomenon is not a consequence of the removal of the RC from the membrane. The source of the multiexponential decay of the primary donor excited state was examined, leading to the conclusion that a distribution in the driving force (ΔG) for electron transfer cannot be the sole parameter that determines the multiexponential character. Further measurements on membrane-bound mutant RC's showed that chemical prereduction of the acceptor quinones resulted in a significant slowing of the rate of primary charge separation. This was most marked in those mutants in which the rate of charge separation had already been slowed down as a result of mutagenesis at the M210 position. The phenomenon is discussed in terms of the Coulombic interaction between Q_A^- and the other pigments involved in electron transfer and the influence of this interaction on the driving force for charge separation.

Introduction

The bacterial reaction center (RC) is an efficient optoelectric cell, which upon absorption of light-energy transfers an electron across the photosynthetic membrane before loss processes (e.g., fluorescence) become important. The crystal structure of the purple bacterial RC has been determined for two species, *Rhodopseudomonas (Rps.) viridis*[1,2] and *Rhodobacter (Rb.) sphaeroides*.[3−5] The *Rb. sphaeroides* RC consists of three subunits, H, L, and M, of which L and M are related by a 2-fold axis of symmetry and bind the cofactors involved in electron transfer. These cofactors, four molecules of bacteriochlorophyll *a* (Bchl-*a*), two molecules of bacteriopheophytin *a* (Bphe-*a*), and two molecules of ubiquinone (Q), are arranged in two branches, but only the "L-branch" is active in electron transfer.[6] The primary electron donor (P) is a pair of Bchl molecules, which lie embedded in the RC protein close to the periplasmic face of the membrane. The formation of the first singlet excited state of the primary donor (P*), either by energy transfer from the antenna or by direct absorption by the RC pigments, triggers the transfer of an electron across the membrane dielectric.

The kinetics of the primary electron transfer have been studied extensively with high time resolution using detergent-solubilized RC's, and the lifetime of P* has been found to be approximately 3.5 ps at room temperature.[7−9] The mechanism of electron transfer from P* to the Bphe molecule (H_L) located halfway across the membrane is still a matter of debate. Two models have been proposed to describe this electron transfer process, which differ in the role played by the monomeric bacteriochlorophyll molecule (B_L), which in the crystal structure bridges the gap between P and H_L. In the sequential model, the state $P^+B_L^-$ is formed as a distinct, but short-lived, intermediate between P* and $P^+H_L^-$,[10−12] while in the superexchange model, $P^+B_L^-$ is a virtual state enhancing the electronic coupling between P* and $P^+H_L^-$.[13,14] A model in which both the sequential and superexchange scheme contribute to the electron transfer proton has also been discussed.[14,15]

In seeking to understand the striking asymmetry of electron transfer in the RC, much attention has been focused on the residue pair Tyr M210/Phe L181 (Tyr M210 in *Rps. viridis* and *Rb. capsulatus*).[8,15,16] These conserved residues are in close contact with P and with the Bchl and Bphe on the active and inactive branches, respectively. As yet the precise role of Tyr M210 and the significance of the conserved Tyr/Phe arrangement are unclear; although the tyrosine has the capacity to form a hydrogen bond, there is no unequivocal evidence that it is H-bonded to P or the pigments on the active branch, with contrasting statements in the literature.[4,17] It has been proposed, on the basis of electrostatic calculations, that Tyr M210 acts to lower the energy of $P^+B_L^-$ relative to that of $P^+B_M^-$, placing the energy of $P^+B_L^-$ in a region consistent with the operation of a sequential model for electron transfer.[18] Alternatively, it

* Corresponding author.
† Department of Physics and Astronomy, Vrije Universiteit.
‡ University of Sheffield.
§ Department of Plant Physiology, Vrije Universiteit. Current address: Department of Biochemistry, University of Pennsylvania, Philadelphia, PA 17104.
⊗ Abstract published in *Advance ACS Abstracts,* April 1, 1996.

0022-3654/96/20100-7256$12.00/0

may enhance the electronic coupling between P* and $P^+H_L^-$ to permit the operation of a superexchange reaction mechanism.[14,18]

In recent years it has become clear that the decay of P* is not a monoexponential process but is described by two exponents with time constants of 2.3−2.9 and 7−12 ps in an approximate 4:1 ratio.[9,19−23] In addition, a subpicosecond component has been reported for isolated RC's from *Rb. sphaeroides* (0.9 ps[10,11]), *Rps. viridis* (0.65 ps[24]), and membrane-bound RC's from *Rb. capsulatus* (0.9 ps[25]) and *Rb. sphaeroides* (1.5 ps[26]). This component has been explained in terms of a sequential electron transfer reaction involving B_L, with the initial charge separated state ($P^+B_L^-$) being formed with the kinetics of P* decay followed by electron transfer within 1 ps from $P^+B_L^-$ to $P^+H_L^-$.

In membranes prepared from WT strains of *Rb. sphaeroides*, the absorbance and energy transfer properties of the light-harvesting antenna complexes are such that the kinetics of charge separation can only be measured following purification of the RC by solubilization in detergent. Although detergent-solubilized WT RC's are relatively stable, it cannot be ruled out that the isolation procedure introduces instabilities or deformations in the structure of the protein that could contribute to the complex kinetics that have been observed, particularly in mutated RC's. Recently, it has become possible to genetically delete the antenna complexes from the membrane of *Rb. sphaeroides*, leaving the RC as the sole pigment protein complex.[27] Measurements of the rate of P* decay in these RC-only membranes have revealed a time constant of 4.5 ps for primary charge separation,[23] in good accord with the results of Schmidt et al.[25] on a similar RC-only mutant of *Rb. capsulatus* and significantly slower than the rate (3.2 ps) in detergent solubilized RC's from the same *Rb. sphaeroides* strain.[23] A detailed comparison of the time-resolved absorbance properties of purified RC's and RC-only membranes, together with an account of the multiexponential nature of P* decay and the effects of chemical reduction of the acceptor quinones on the kinetics of P* decay in the different preparations, is given in a recent paper.[23]

Here we focus upon the kinetics of charge separation in membrane-bound RC's bearing mutations at the L181 and/or M210 positions and compare our results with the detailed analyses that have been presented by others of the kinetics of P* decay in detergent-solubilized RC's with the same mutations.[9,15,16,22,28,29] Furthermore, we examine in more detail the effects of quinone reduction on the kinetics and multiexponentiality of P* decay and discuss the origin of these effects. We will relate the multiexponential decay of P* observed in these systems to the classical nonadiabatic electron transfer theory[14,30] and discuss whether our data may be described in terms of a distribution in the driving force ΔG for the primary electron transfer step.

Materials and Methods

Mutant Construction and Sample Preparation. The construction of the mutants bearing changes at the M210 position to Phe, His, and Leu has been described previously.[31] The changes Tyr M210 → Trp and Phe L181 → His were made in a similar manner, using in the case of the latter a 0.85-kb *Xba*I-*Sal*I restriction fragment as the template for mutagenesis. Codon changes were TTC → CAC (Phe L181 → His) and TAC → TTC (Tyr M210 → Trp). The following nomenclature for the mutant strains will be used throughout: WT, RC-only strain with WT RC's; YM210F, TyrM210 → Phe; YM210L, TyrM210 → Leu; YM210H, TyrM210 → His; YM210W, TyrM210 → Trp; YM210H/FL181H, TyrM210 → His/PheL181 → His double mutant. The basis for the deletion and expression systems used to construct mutants with an RC-only phenotype is described in detail in ref 27. The growth of mutant *Rb. sphaeroides* strains and preparation of membranes for spectroscopy are as previously described.[31] All spectroscopic measurements were performed on intracytoplasmic membranes in a buffer containing 50 mM Tris, 10 mM EDTA (pH 7.8).

Time-Resolved Spectroscopy. Transient absorption difference spectra were measured as described elsewhere.[23,32] Briefly, the instrument consisted of a mode-locked Nd-YAG laser (Antares, Coherent) that was used to synchronously pump a hybrid dye laser (Satori, Coherent) with intracavity group velocity dispersion (GVD) compensation, yielding 200-fs pulses at 590 nm. The pulses were then amplified to an energy of 0.5 mJ/pulse at a repetition rate of 30 Hz by using a regenerative doubled Nd-YAG amplifier and a three stage dye amplifier. The beam was split into an excitation beam (5%), which was put through a variable optical delay, and a detection beam (95%) that was used to create a white light continuum by focusing the beam into a flowing water cell. The white light continuum was passed through a pair of prisms to compensate for GVD and was split into two equal parts, one of which was used to probe the excited spot in the sample and the other as a reference. Both beams were projected onto a double diode-array detector, giving 130-nm-wide spectra. The chirp compensation was tuned to be optimal by changing the amount of prism in the pathway of the beam and measuring the birefringence signal of CS_2 between two crossed polarizers.[32]

Time-resolved spectra were measured over two spectral regions (720−850 nm and 815−945 nm) and the GVD compensation was optimized for both regions separately. Tuning the GVD compensation has two disadvantages for combining spectra from the two spectral regions. GVD compensation was achieved by altering the amount of prism in the probe beam, which introduced a slight time shift, ∼500 fs, of the spectral data sets with respect to one another. Furthermore, as the GVD compensation affects the path of the beam, it can alter the profile of the white light probe-beam which, in turn, can introduce slight variations in the overlap of pump and probe beam (i.e., the overlap with different colors may have changed slightly). If the chirp compensation was taken out, as was done for measurements on a long time-scale, both effects disappeared. The measurements were performed in a 1-mm rotating cell to ensure that each pulse excited a new region of the sample. The optical density of the samples of RC-only membranes was between 0.3 and 0.25 mm^{-1} at 860 nm. The excitation density was tuned to be approximately 30%, giving rise to an absorption difference at 860 nm of approximately 0.08. Due to the relatively low absorption of the sample of RC-only membranes, about 2000−3000 flashes were averaged in order to obtain spectra with reasonable signal-to-noise characteristics. Absorption differences down to approximately 0.005 could be measured accurately.

Two color pump-probe measurements of the decay of stimulated emission from P* (920 nm) and H_L^- formation/loss (680 nm) were performed by using an amplified high repetition rate (25−250 kHz) Ti−sapphire system (Mira-Rega, Coherent). The amplified pulse (at 800 nm) was split into two, the larger part of which was used to create a stable white light continuum, and the smaller part of which was passed through an optical delay and then through the sample as the pump pulse. The detection wavelength was selected by using band-pass filters centered at either 920 or 680 nm. After passage through a

monochromator to reduce scatter from the excitation pulse, the detection beam was measured by using a photodiode, and the signal was filtered out by using a lock-in amplifier.

In order to avoid the buildup of large fractions of RC's in the closed ($P^+Q_A^-$) state during measurement with the high repetition rate laser system, three incubation conditions were employed. In the first, the acceptor quinone Q_A was prereduced by adding 200 mM sodium ascorbate to the sample of RC-only membranes, leading to recombination to the state $^3PH_LQ_A^-$ in approximately 20 ns followed by recovery of the ground state after a few microseconds, by quenching of the triplets by the carotenoids present in the RC's. Experiments with WT RC-only membranes showed that essentially identical results could be obtained if Q_A was prereduced by using sodium dithionite. Under such conditions we could employ repetition rates as high as 250 kHz (4-μs interval between pulses). We also used a combination of 500 μM phenazine methosulphate (PMS) and 100 μM cytochrome *c* to keep RC's in the open state (PH_LQ_A) by accelerating the rate of P^+ reduction and Q_A^- oxidation. Under these conditions the repetition rate of the laser was set at 25 kHz, with the RC-only membranes housed in a rotating cell.

Global Analysis and Kinetic Fits. Analysis of the time-resolved absorption difference spectra obtained with the 30-Hz system was performed using a Global analysis program as described in ref 33. To determine the number of spectrally and temporally distinct components a singular value decomposition was used. Compartmental models were used to analyze the data in terms of the kinetics of the RC. The use of an all parallel model gives rise to decay associated spectra (DAS), in which the amplitude of each decay time is given at each wavelength. In case of the bacterial RC, a sequential kinetic model with four compartments yields spectra for the intermediates B*, P*, $P^+H_L^-$, and $P^+Q_A^-$. These spectra are no longer associated with a single decay component but with a state in the kinetic model and are referred to as species associated spectra (SAS).

In the Global analysis of the data acquired with the 30-Hz system, the two spectral regions were analyzed simultaneously. The instrument response is well described by a Gaussian with parameters for location and width. A time shift was fitted between the two spectral data sets to account for the time shift due to GVD compensation, discussed above. Thus the model describing the two spectral regions contained seven nonlinear parameters: four rate constants, the width of the instrument response, and its location for each spectral region. The DAS or SAS are conditionally linear parameters.[33]

The single wavelength data recorded with the high repetition rate system were analyzed using a nonlinear least squares fitting program which convoluted the decay with a Gaussian profile that described the instrument response well. A maximum of two exponential decay terms were fitted together with a nondecaying part, which was added to account for absorbance changes that were constant on the time scale of the measurement (i.e., such as those arising from P^+ formation). The data were also analyzed with a distribution of rate constants, the distribution was a Gaussian on a (natural) logarithmic rate scale (ln(k)) and is characterized by a central rate (k_c) and a width (σ). Thus the fit function is described by

$$\int_{-\infty}^{\infty} \exp\left[-\frac{(\log(k)-\log(k_c))^2}{2\sigma^2}\right]\{\exp(-kt)\otimes i(t)\}\, \mathrm{d}\log(k) \quad (1)$$

Where the first term describes the distribution of log(k) and the second term the convolution ($\otimes$) of the decay with the instrument response ($i(t)$), the above-mentioned Gaussian profile. Thus the models describing a single wavelength contained three or four nonlinear parameters: location and width of the instrument response and either one or two rate constants or the pair (k_c, σ) describing the distribution from eq 1. The amplitudes of the exponential terms and of the nondecaying part are again conditionally linear parameters.

Steady-State Absorption Spectroscopy, Linear Dichroism Measurements, and Redox Potentiometry. Room and low temperature absorption spectroscopy, light-minus-dark difference spectroscopy, and linear dichroism measurements were performed on a laboratory-built spectrophotometer described previously.[34] For measurements of linear dichroism, samples were oriented in gelatin gels by compression along two horizontal axes with expansion along the vertical axis. The $A_{\parallel} - A_{\perp}$ was measured by varying the polarization of the measuring beam at a frequency of 100 kHz with a photoelastic modulator and detecting the resulting signal with a lock-in amplifier. For measurements of light-minus-dark difference spectra the actinic source was a continuous Ti:sapphire laser emitting at 800 nm. Equilibrium titrations of the electrochemical midpoint potential of the P/P^+ redox couple were performed as described in ref 23.

Results

Steady-State Absorption and Linear Dichroism Spectra. The Q_y region of the room temperature ground state absorbance spectra of membranes from the WT RC-only strain and the YM210H and YM210F mutant strains is shown in Figure 1A. The mutations have little effect on the position or intensity of the absorbance band of P (at 860 nm), apart from a slight red-shift in the YM210F mutant. In the region around 800 nm, where the absorbance is dominated by contributions from the monomeric Bchls, a small red-shift of the absorption maximum was observed from 800 to 802 nm in the YM210F and YM210H mutants, and a similar effect was seen in spectra of the YM210L, YM210W, and YM210H/FL181H mutants (data not shown). This shift is comparable to that reported by other groups for isolated RC's[28,29,35] and for membrane-bound RC's in the presence of the LH1 antenna complex.[36]

In the Bphe absorbance region a large (10−20 nm) red-shift and broadening of the 760-nm absorbance band was seen in both mutants where the M210 residue was altered to a His (YM210H and YM210H/FL181H). On lowering the temperature to 77 K this broadened absorption band was seen to split into two distinct bands (Figure 1b) as has been reported previously for the YM210H mutant at 20 K.[31] This splitting of the Bphe absorbance bands has been attributed to the formation of an H-bond between the Bphe on the active branch (H_L) and the His residue at position M210.[31,37]

To investigate the Q_y-Bphe absorption band in more detail, linear dichroism (LD) measurements at 77 K were performed. The OD, LD, and LD/OD spectra of the YM210H mutant (Figure 2A) all clearly show the splitting of the Bphe band. On the basis of the LD/OD spectrum (Figure 2A) it would appear that the Q_y transition of the red-most absorbing Bphe-pigment (assigned as H_L) is tilted more out of the plane of the membrane than that of H_M (i.e., it makes a smaller angle with the C_2 axis of symmetry). From the spectrum we estimate that there is a difference in the angle that the Q_y transitions of H_L and H_M make with the C_2-symmetry axis of 4−5°. The average orientation of the two Bphe transitions in YM210H, estimated from LD/OD spectra, was similar to that calculated for WT and YM210F where the H_L and H_M transitions are not resolved (Figure 2B, Table 1). From this similarity we infer that the difference of 4−5° between the transition dipoles calculated

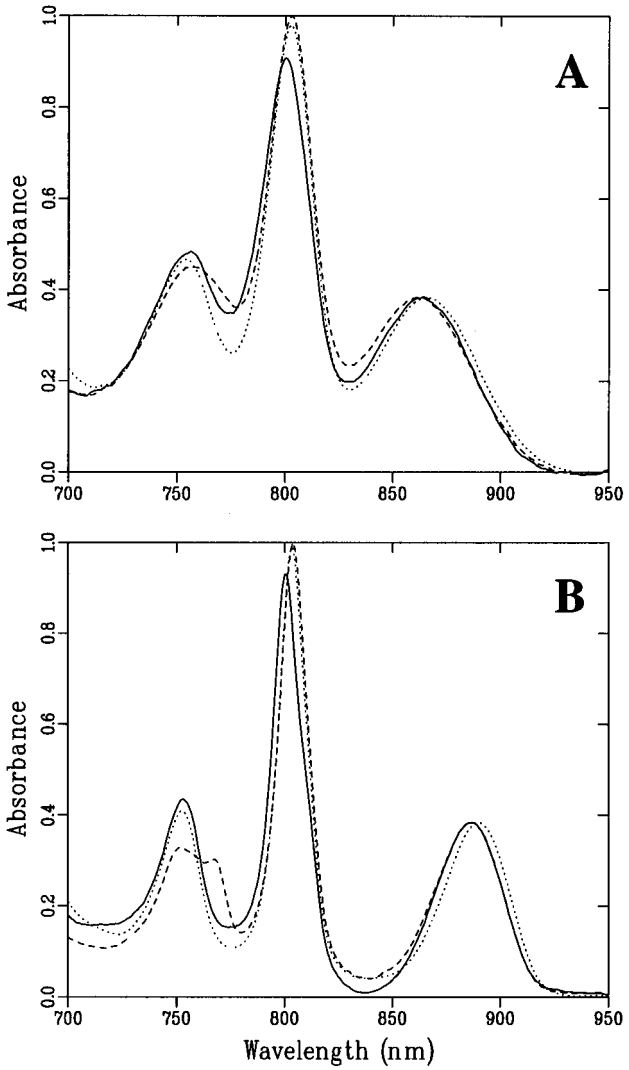

Figure 1. Near-infrared absorption spectrum at room temperature (A) and 77 K (B) of RC-only membranes from WT (solid), YM210F (dot), and YM210H (dash).

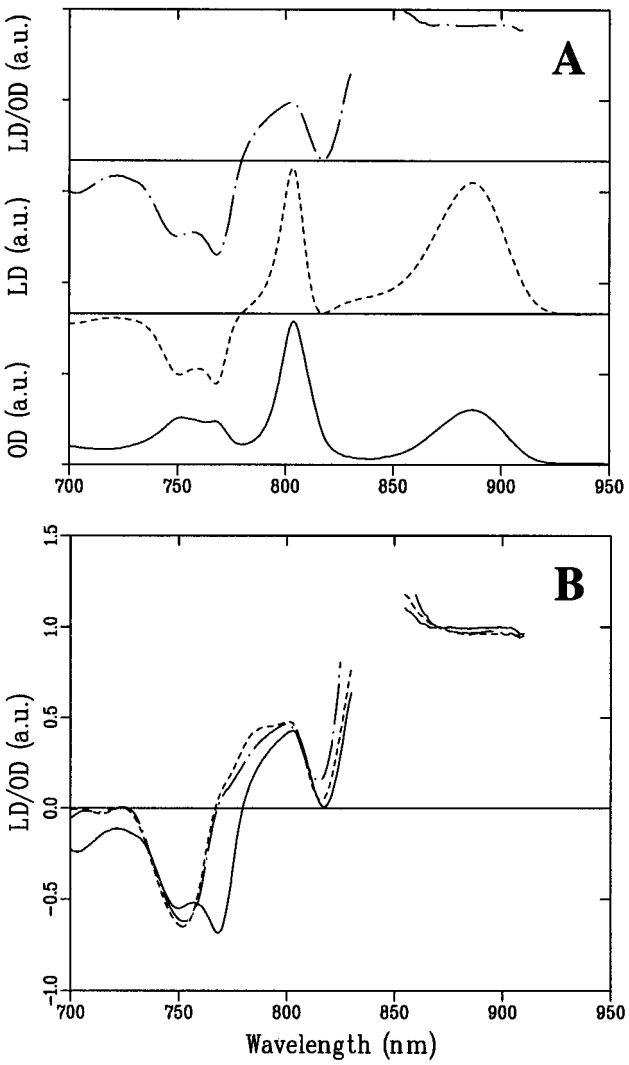

Figure 2. (A) 77 K absorption spectrum (solid) of YM210H together with LD (dash) and LD/OD (chain dot) spectra. (B) The LD/OD spectra of WT (chain dot), YM210F (dash), and YM210H (solid) are compared.

from our data on the YM210H mutant is also present in RC's of the WT strain. This difference may be compared with the value of 5° estimated from the crystal structure of *Rps. viridis*.[38,39]

Spectral Evolution and Rates of Primary Charge Separation. Figure 3A shows the time evolution of the absorbance difference spectrum for RC-only membranes containing WT RC's, recorded by using the 30-Hz multiple wavelength pump-probe system. The excitation wavelength of 595 nm used in this experiment was such that all four Bchl pigments of the RC were excited (in their Q_x transitions). The principle feature in the earliest spectrum recorded after the pump pulse were bleaches at approximately 800 and 870 nm (Figure 3A; solid line), which are ascribed to excitation of the monomeric Bchl molecules and P, respectively. Following rapid (<400 fs) energy transfer from the monomeric Bchls to P, changes in the absorbance difference spectra were observed over the next 40 ps that are characteristic of primary charge separation. These were the loss of the stimulated emission band on the red side of the bleach of the P ground-state band as P* decays to P^+, a bleach of the Q_y transition of H_L at around 760 nm as H_L is converted to H_L^-, and a progressive blue-shift of the 800-nm band of B_L and B_M in response to the development of the electric field from P^+ and H_L^-. The bleach of the ground-state absorbance band of P and the broad, low amplitude absorbance increase across the 720−945 nm attributed to P^+ were permanent on the time scale of our measurements. The spectrum recorded 700 ps after excitation (Figure 3A; dotted line) showed evidence of the secondary step of electron transfer from H_L^- to Q_A, specifically a decrease in the amplitude of the 800-nm band-shift in response to the decrease in the strength of the electric field as $P^+H_L^-$ is converted to $P^+Q_A^-$ and a red-shift of the Bphe absorbance band in response to the electric field between P^+ and Q_A^-.

TABLE 1: Angles of the Transition Dipoles, Estimated from LD/OD Spectra

mutant	P (860),[a] θ_1	P (810),[b] θ_2	B, θ_3	H_L, θ_4	H_M, θ_5
wild-type	0°	53.0°	45°	71°	
YM210 → H	0°	54.7°	46°	72°	68°
YM210 → F	0°	54.7°	45°	71°	

[a] For the low exciton component of P absorbing at 860 nm at room temperature the angle is fixed to 0°, based on the crystal structure. [b] The high exciton component of P is perpendicular to the low exciton component but carries only about 10% of the oscillator strength. We find an almost magic angle (54.7°) value for the orientation due to overlap with the B band.

Figure 3B,C shows data for YM210H/FL181H and YM210L, respectively. The same features indicative of primary electron transfer were observed. Spectra recorded for YM210F, YM210W, and YM210H were also very similar in their overall features (data not shown).

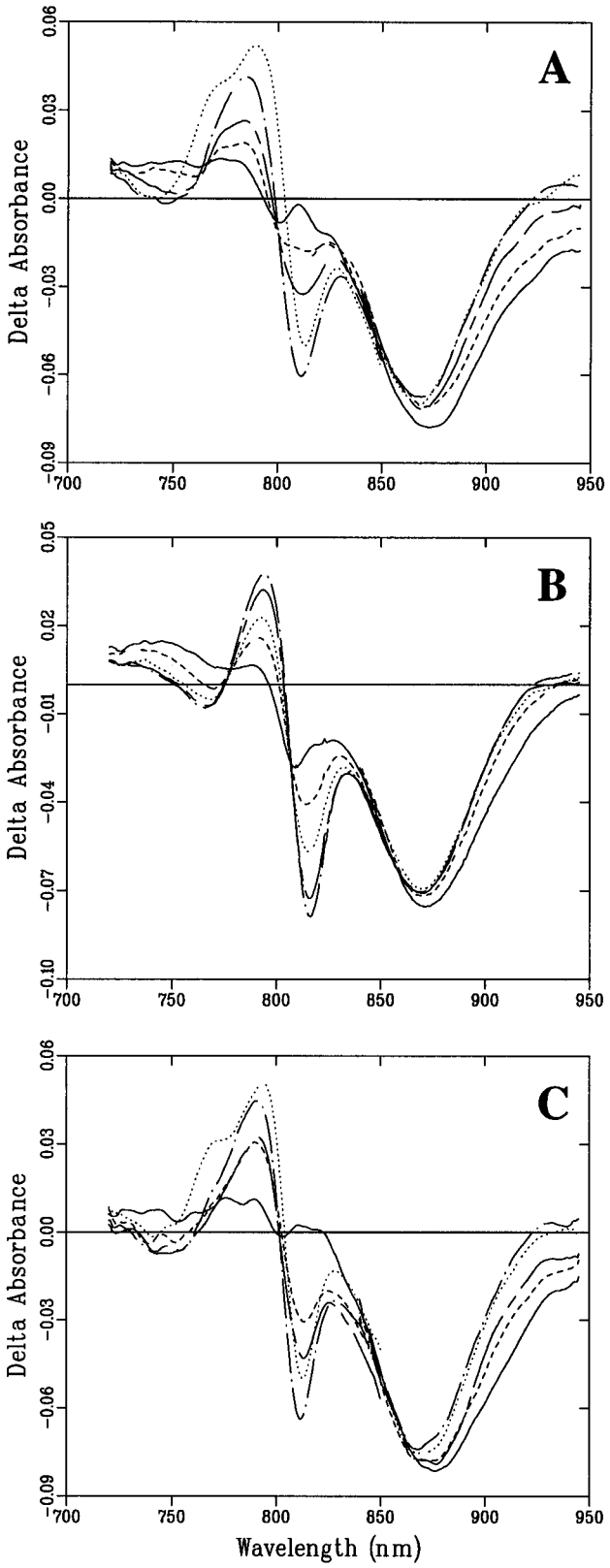

Figure 3. Time-resolved absorption difference spectra for WT and two mutant RC-only membranes. (A) WT taken at 0.5 (solid), 2 (dash), 5 (chain dash), 40 (chain dot), and 700 ps (dot) after excitation. (B) YM210H/FL181H: 0.83 (solid), 2.5 (dash), 4.2 (dot), 7.5 (chain dash), and 11.6 ps (chain dot) after excitation. (C) YM210L: 2 (solid), 20 (dash), 40 (chain dash), 130 (chain dot), and 730 ps (dot) after excitation.

Global Analysis of the Time-Resolved Spectra. The singular value decomposition of the time-resolved difference spectra indicated that for each of the mutants, depending on the time scale of measurement, three or four spectrally and temporally distinct components were required to describe the data. This implies a kinetic model with at least three of four compartments. We performed a Global analysis with a sequential reaction scheme with the thus determined number of compartments. In Figure 4 we show the SAS of the P* (solid), $P^+H_L^-$ (dashed), and $P^+Q_A^-$ (chain-dot) intermediates; the B* spectrum is not shown. In the case of the YM210H mutant (B) due to the limited time window of 12 ps the secondary electron transfer step was not observed. Therefore in Figure 4B only two SAS are depicted. The general features of the SAS calculated from this analysis were similar for the WT RC-only membranes and for the mutants (Figure 4), in particular two different electrochromic band shifts are clearly visible. Details of the P* spectra will be considered in the Discussion. In Table 2 column 3, we list the time constants for decay of P* derived from the Global analysis. The values obtained are in general agreement with time constants determined for detergent-solubilized, mutated RC's from *Rb. sphaeroides* and *Rb. capsulatus* by other groups (Table 4), with the rate of charge separation being slowed down.

Two Color Pump-Probe Measurements of the Rate of P* Decay. The decay of stimulated emission recorded at 918 nm following excitation at 800 nm for RC-only membranes of the WT and the mutants is shown in Figure 5. In these experiments a combination of PMS and cytochrome *c* was used to maintain the RC's in an open state during measurements with the high repetition rate laser. The higher time resolution and signal to noise ratio of all the stimulated emission traces enabled us to compare fits with one or two exponential decays. In most cases a biexponential decay provided the best fit to the data (Table 5, columns 4 and 5). In Table 3 we list two sets of time constants derived from the single wavelength data. The results of the (unsatisfactory) monoexponential fits to the data give a mean decay time of P* (τ) and provide a comparison to the data acquired with the 30-Hz system. The results of the biexponential fit to the data (τ_1 and τ_2) are also shown in Table 3, together with the percentage amplitudes.

From Tables 2 and 3 it seems as if the overall rate of P* decay as measured by the monoexponential fit (Table 3) is slower than obtained from the Global analysis (Table 2). This is only an apparent effect and is caused by the limited time-window of the latter data (see Discussion). The trend of a progressive slowing of the charge separation rate in the order YM210F, YM210L, YM210W is evident in both data sets.

A feature that is clearly evident from the data summarized in Tables 2 and 3 is that the single wavelength data suggested variation in relative amplitudes of the fast and slow components in the two component fits (Table 3). In those RC's where charge separation was most rapid (the WT complex and the YM210H/FL181H mutant), the slow component represented 16−17% of the overall amplitude of P* decay. In the mutants, where the overall rate of charge separation was slower than the WT, the amplitude of this component represented between 37% and 63% of the overall decay. Note that although on the basis of the monoexponential fit the overall rate of charge separation in YM210H was slower than in either WT or YM210H/FL181H (5.8 ps c.f. 4.8 ps and 4.3 ps respectively), the fast component in the biexponential fit of YM210H (2.7 ps) was more rapid than the corresponding components in the fits for WT and YM210H/FL181H (3.7 and 3.1 ps, respectively). This acceleration in the rate of charge separation, which was also manifested in the time constants for the slower components (7.5 ps, cf. 11.9 and 11.3 ps), was masked by a significant increase in the relative amplitude of the slow component in YM210H (from

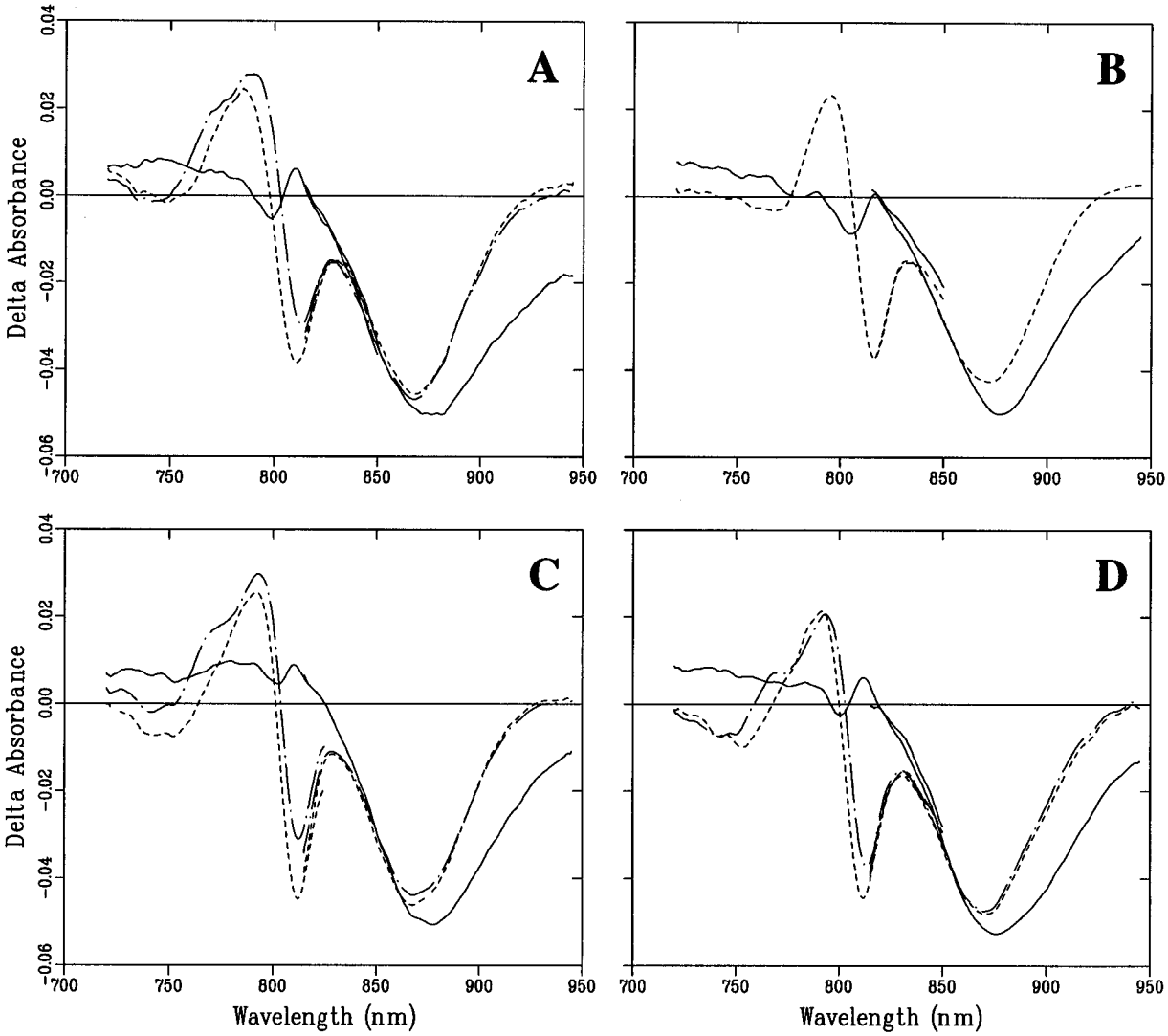

Figure 4. SAS obtained from global analysis of time-resolved difference spectra for (A) WT, (B) YM210H, (C) YM210L, and (D) YM210F mutants. The spectra corresponding with different states in the sequential model for electron transfer are P* (solid), $P^+H_L^-$ (dash), and $P^+Q_A^-$ (chain-dot).

TABLE 2: Redox Potentials and Decay Times for the Primary and Secondary Reaction

mutant	P/P^+, mV	$P^* \rightarrow P^+I^-$,[a] *t*, ps	$I^- \rightarrow Q_A^-$,[a] *t*, ps	$I^- \rightarrow Q_A^-$,[b] *t*, ps
wild-type	495	4.5	175 ± 30	213 ± 40
YM210 → H	422	3.5	300 ± 30	
FL181 → H				
YM210 → H	457	4.2		270 ± 40
YM210 → F	528	24	230 ± 30	215 ± 40
YM210 → L	526	36	250 ± 30	270 ± 40
YM210 → W	549			250 ± 40
wild-type (isolated)	487	3.3		180 ± 40

[a] Time constants obtained from global analysis of transient absorption spectra. [b] Secondary electron transfer time measured at 690 nm under PMS/Cyt-*c* conditions with a 25-kHz repetition frequency of the laser system.

16% in WT to 60% in YM210H). We note that most of the differences are probably not significant and may merely reflect some variation in the outcome of the two component analysis.

Effect of Chemical Reduction of the Acceptor Quinones on the Rate of Charge Separation. As an alternative to PMS/cytochrome-*c*, sodium ascorbate may be used to keep the RC's in an active state during the two color pump-probe measurements with the high repetition rate laser system. Ascorbate reduces the acceptor quinones (Q_A and Q_B), leading to rapid (~20 ns) charge recombination from $P^+H_L^-$ rather than slower (100 ms) recombination from $P^+Q_A^-$ in untreated complexes. In a recent paper,[23] we demonstrated that chemical reduction of the acceptor quinones leads to a slight slowing down of the rate of P* decay in WT membrane-bound RC's. The effect of prior reduction of the Q_A quinone on the rate of charge separation in the mutated complexes, summarized in Table 3, was slowing in the rate of charge separation and was most marked in the slower mutants (YM210L and YM210W).

Secondary Electron Transfer from H_L^- to Q_A. In order to examine the influence of mutation on secondary electron transfer from $P^+H_L^-$ to $P^+Q_A^-$ we used the high repetition rate laser system to monitor the formation and decay of H_L^- at 680 nm.[10,11] From the Global analysis of time-resolved spectra on a long (700 ps) time scale we have also obtained a value for the secondary electron transfer process for WT, YM210H/FL181H, YM210L, and YM210F. The results of these experi-

TABLE 3: Stimulated Emission Decay in Membrane-Bound Reaction Centers

				ascorbate[c]					
mutant	Cyt, PMS,[a] τ, ps	Cyt, PMS,[b] τ_1	(a_1)	τ_2	(a_2)	τ_1	(a_1)	τ_2	(a_2)
wild-type	4.82 ± 0.04	3.67 ± 0.12	(84)	11.9 ± 1.2	(16)	4.04 ± 0.17	(75)	13.3 ± 1.0	(25)
YM210H/FL181H	4.32 ± 0.15	3.1 ± 0.5	(84)	11.3 ± 4.5	(16)*	2.5 ± 0.15	(70)	11 ± 0.9	(30)
YM210H	5.81 ± 0.06	2.7 ± 0.4	(40)	7.5 ± 0.4	(60)	3.77 ± 0.17	(67)	17.9 ± 1.4	(33)
YM210F	27.7 ± 0.3	15.3 ± 1.5	(45)	38.5 ± 2.4	(55)				
YM210L	37.9 ± 0.3	26.3 ± 2.0	(63)	65 ± 9	(37)	26.7 ± 4	(39)	103 ± 6	(61)
YM210W	72.5 ± 0.7	31.7 ± 3.3	(37)	97.5 ± 4.5	(63)	100 ± 7			

[a] Analysis with single exponential decay, incubation conditions Cyt-*c* and PMS. [b] Same traces as now analyzed by using a biexponential decay. [c] Analysis with biexponential decay, prereduced quinones by addition of ascorbate.

TABLE 4: Comparison of Rate of Decay of Fluorescence Emission from P* in Membrane-Bound RC's with Published Data on Solubilized RC's

			membrane-bound RC's[b]		solubilized RC's[b]			
mutant	species	source[a]	monoexponential	biexponential	monoexponential	biexponential	ΔE_m,[c] mV	method
wild type	*Rb. sph*	this work	4.8	3.6 (80) 12 (20)				stim emiss
	Rb. sph	B (1995)			4.1	3.2 (85) 13 (15)		stim emiss
	Rb. sph	N (1993)			3.5			Global anal.
	Rb. sph	H (1993)				2.3 (80) 7 (20)		spont emiss
	Rb. caps	C (1991)			3.5			stim emiss
	Rb. caps	J (1993)			2.8			stim emiss
	Rb. caps	J (1993)				2.7 (72) 11 (28)		spont emiss
H M210/	*Rb. sph*	this work	4.2	2.8 (75) 9.3 (25)			−73	stim emiss
H L181	*Rb. caps*	J (1993)			4.4		−55	stim emiss
H M210	*Rb. sph*	this work	5.8	2.5 (40) 8.2 (60)			−38	stim emiss
	Rb. caps	C (1991)			3.7			stim emiss
	Rb. caps	J (1993)			3.9		−36	stim emiss
F M210	*Rb. sph*	this work	28	15 (42) 38 (58)			+33	stim emiss
	Rb. sph	N (1993)			11		+30	Global anal.
	Rb. sph	H (1993)				6.1 (42) 26 (58)		spont emiss
	Rb. sph	F (1990)				16 (75) 70 (25)		stim emiss
	Rb. caps	C (1991)				9.2 (80) 126 (20)		stim emiss
	Rb. caps	J (1993)				5.4 (53) 40 (47)	+11	spont emiss
L M210	*Rb. sph*	this work	36	24 (55) 62 (45)			+31	stim emiss
	Rb. sph	F (1990)				22 (75) 90 (25)		stim emiss
W M210	*Rb. sph*	this work	72	32 (35) 98 (65)			+54	stim emiss
	Rb. sph	N (1993)			41		+52	Global anal.
	Rb. sph	S (1994)				5.1 (20) 36 (80)		stim emiss

[a] Relevant references are: B (1995), Beekman et al. (1995);[23] C (1991), Chan et al. (1991);[15] F (1990), Finkele et al. (1990);[18] H (1993), Hamm et al. (1993);[9] J (1993), Jia et al. (1993);[28] N (1993), Nagarajan et al. (1993);[33] S (1994), Shochat et al. (1994).[34] [b] Time constants for mono- or biexponential kinetics of P* decay with amplitudes for biexponential decays expressed as percent of total decay. [c] Change in E_m for the P/P^+ redox couple relative to value determined for wild-type complex in the same study.

ments are summarized in Table 2 (columns 5 and 4, respectively). In contrast to the results for primary charge separation, no clear trend in the effect of the site-directed mutations on the rate of secondary electron transfer to Q_A was observed and all time constants ranged between 200 and 300 ps. Interestingly, however, the slowest rates were found in YM210H and YM210H/FL181H, where there is clear evidence of an influence of the residue at the M210 position on the properties of H_L, manifested in the red-shift of the absorption spectrum of this pigment. This may be an indication of a change in the H_L/H_L^- redox potential which would alter the driving force for the secondary electron transfer step.

Discussion

Tyr M210 occupies a key position in the RC in close proximity to the four bacteriochlorin pigments that participate in the primary electron transfer reaction. In the following we will examine evidence for possible influences of this residue on the properties of the surrounding pigments. This will be discussed in the context of the effects that mutations at the M210 and L181 positions exert on the spectral features of the RC and the kinetics and energetics of primary and secondary electron transfer.

Steady-State Optical Properties of the Membrane-Bound, Mutated RC's. The room temperature absorption spectra of the membrane-bound, mutated RC's provide evidence for an influence of the M210 residue on the optical properties of both the accessory Bchl and Bphe in the active pigment branch. As has been reported previously by others for detergent solubilized RC's, removal of the Tyr M210 induces a 2−3-nm red-shift in the position of the absorption maximum of the monomeric Bchl band (at ∼800 nm).[28,29,31,35] At low temperature, the spectrum of the WT complex displays a distinct shoulder on the red side of this band which has been assigned to B_M[40] and which is probably resolved as the result of an asymmetry between B_L and B_M. Spectra recorded for membrane-bound RC's of YM210F and YM210H at low temperature lack the structure on the 800-nm absorbance band and have a red-shifted absorbance maximum, consistent with a red-shift of the B_L absorption band. Similar results were obtained with YM210L, YM210W, and YM210H/Fl181H. These observations are in full accord with results obtained for detergent-solubilized YM210H, YM210L, and YM210F RC's at 20 K.[31]

The most striking feature of the spectra shown in Figures 1 and 2 is the splitting of the Bphe absorbance band in YM210H, which is particularly pronounced at low temperature. This splitting has been reported previously for detergent-solubilized YM210H RC's[31] and for the same mutant in *Rb. capsulatus*[37] and probably arises as a result of the formation of an H-bond

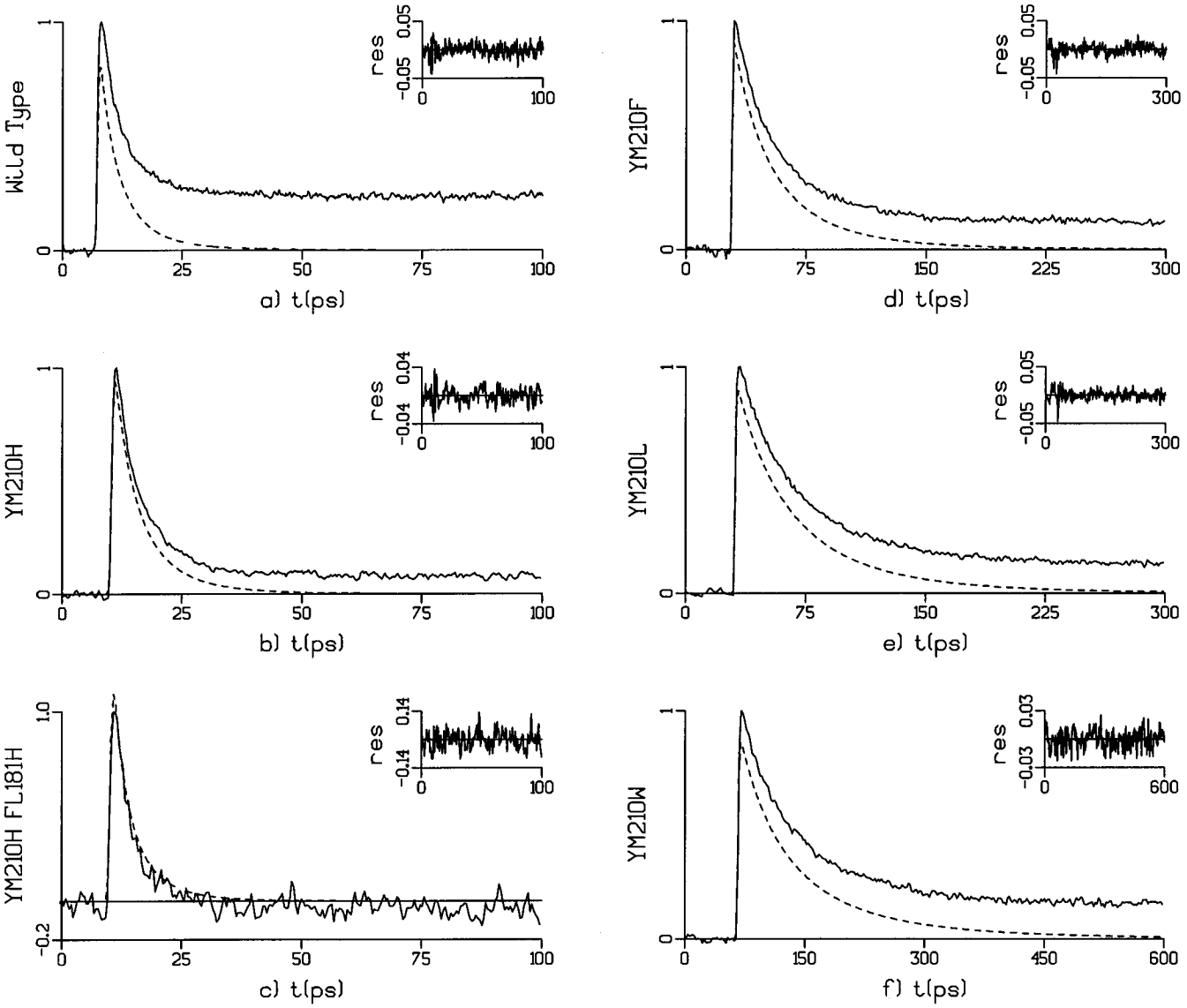

Figure 5. Stimulated emission decay of P* recorded at 918 nm for RC-only mutants. The dashed curves in the plots represent the decaying part of the fit with a distribution as given by eq 1; the parameters of the fits are given in Table 5. The insets are the residuals of the fit with a distribution.

TABLE 5: Fit of Stimulated Emission with a Gaussian Distribution

			$\chi^{2\,a}$		
mutant	distribution, τ, ps	$\sigma(\ln(k))$	1-exp	2-exp	distribution
Wild-type	$\tau = 4.17 \pm 0.07$	$\sigma = 0.52 \pm 0.03$	0.280	0.231	0.237
YM210H/FL181H	$\tau = 3.5 \pm 0.4$	$\sigma = 0.56 \pm 0.11$	0.455	0.445	0.445
YM210H	$\tau = 5.1 \pm 0.1$	$\sigma = 0.48 \pm 0.03$	0.69	0.58	0.58
YM210F	$\tau = 25.6 \pm 0.73$	$\sigma = 0.48 \pm 0.03$	0.224	0.189	0.190
YM210L	$\tau = 36.0 \pm 0.3$	$\sigma = 0.47 \pm 0.02$	0.262	0.201	0.201
YM210W	$\tau = 66.7 \pm 0.8$	$\sigma = 0.58 \pm 0.03$	0.53	0.393	0.398
wild-type[b] (isolated)	$\tau = 3.41 \pm 0.06$	$\sigma = 0.60 \pm 0.03$	0.126	0.084	0.090

[a] The χ^2 values found for a fit to the stimulated emission data of a single exponential decay (1-exp, Table 3, column 2), a biexponential decay (2-exp, Table 3, columns 3 and 4), and a Gaussian distribution (Table 5, column 2 and 3). [b] These data were presented in ref 28.

from the histidine at the M210 position to the 2-acetyl carbonyl group of H_L.[31,37]

The 77 K LD and LD/OD results on WT, YM210H, and YM210F (Figure 2) provide information on the orientations of the transition dipoles of the RC pigments which may be related to the *Rb. sphaeroides* crystal structure.[38,39] It is evident from the LD/OD spectrum of membranes of the YM210H mutant that the Q_y transition of the blue-most Bphe pigment (assigned to H_M) makes a larger angle with the C_2-symmetry axis of the sample than the Q_y transition of H_L. We have calculated the angles between transition dipoles from LD/OD spectra, assuming that the Q_y transition of P lies in the plane of the membrane (Table 1). Since the average orientation of the H_L and H_M Q_y bands of both WT and YM210F is similar to the average orientation of the two Bphe-Q_y transitions in YM210H, we conclude that this difference is also present in the WT complex. This may amongst others be a reason for the directionality of electron transfer.

Electron Transfer from H_L^- to Q_A. The measurements of secondary electron transfer from $P^+H_L^-Q_A$ to $P^+H_LQ_A^-$ provide

further evidence that, in addition to exerting an effect on the redox properties of P, mutations of YM210 also influence the redox properties of H_L. So, for example, there was an approximately 50% slowing down of the rate of secondary electron transfer in YM210H where, as discussed above, there is evidence for the formation of an H-bond to the 2-acetyl carbonyl group of H_L. This effect cannot be explained in terms of a change in the E_m for P/P^+ in this mutant, as this change should affect the free energy of both $P^+H_L^-Q_A$ and $P^+H_LQ_A^-$ to an equal extent. By simple analogy with the results of Allen and co-workers,[41] the creation of a new H-bond from His M210 to the 2-acetyl carbonyl of H_L would be expected to raise the E_m for the H_L/H_L^- redox couple (by approximately 80 mV), making H_L easier to reduce and thus lowering the free energy of $P^+H_L^-Q_A$. The temperature independence of the $P^+H_L^-Q_A \rightarrow P^+H_LQ_A^-$ reaction suggests that the electron transfer reaction is activationless in the WT RC. Therefore a decrease in the driving force for secondary electron transfer in the mutant complex should result in a slower rate of electron transfer,[42] as observed in YM210H.

The significant reductions in the rate of secondary electron transfer in YM210W and YM210L may also be rationalized in terms of an effect on the redox properties of H_L, although we have no direct evidence for this (and the optical properties of H_L in these mutants are not significantly affected by the mutation). However, the data on the E_m for P/P^+ presented in Table 1 shows clearly that, even in the absence of hydrogen bonding effects, it is possible to modulate the midpoint potential of P over a range of nearly 130 mV through mutation at the M210 position. Therefore, it is entirely feasible that the mutations in YM210W and YM210L could also result in a change in the E_m for H_L/H_L^-, although it is not possible to predict whether this would be an increase or decrease on the basis of the observed effect on the rate.

It is worth noting that the amplitude of the signal decay at 680 nm provides a measure of the fraction of RCs that have a reduced Q_A under the incubation conditions (PMS/cytochrome *c*) used to keep the RC's in an open state. A population of RC's in which Q_A was reduced would exhibit a long-lived (20 ns) $P^+H_L^-$ state. From the decay and the maximum amplitude of the signal at 680 nm we can state with confidence that the combination of PMS and cytochrome *c* provides us with RC's that are maintained in an open (PH_LQ_A) state during interrogation with the high repetition rate laser, with less than 10% of the Q_A quinones becoming reduced during the course of the experiment.

Transient Spectral Properties of Membrane-Bound, Mutated RC's. The time resolved difference spectra recorded from 720−945 nm were satisfactorily described by a three or four compartment model. This model also fits data collected previously on both solubilized and membrane-bound forms of the WT RC and is described in detail in a previous paper.[23] In brief, the model takes into account significant (>50%) excitation of B_L and B_M in addition to direct excitation of P and rapid (∼300 fs) energy transfer from B* to P (to form P*). The energy transfer process is modeled as an independent component preceding the charge separation process:

$$B^* \rightarrow P^* \rightarrow P^+H_L^- \rightarrow P^+Q_A^-$$

This energy transfer phase could in principle influence the time constant of P* decay since part of the RC population has B* as the starting state and the remainder will have P*. However, even for the fastest RC's the time scales of the two processes are well separated (∼300 fs vs 4 ps) so any influence is expected to be very small. Our analysis did not reveal the formation of $P^+B_L^-$ as a spectrally-resolvable intermediate, but this should not be taken as an argument against the involvement of $P^+B_L^-$. Such a state would give rise to an absorption difference spectrum in which the ground state Q_y absorbance bands of both P and B_L would be bleached, with an additional electric field effect on the remaining pigments. However, the bleaching of the B band on reduction is very similar to the bleaching that occurs on the formation of B*, which in our experiments is generated in significant quantities by the 590-nm excitation pulse. The lifetime of B* (∼300 fs) is comparable to that reported by Zinth and co-workers[10−12] for the lifetime of $P^+B_L^-$ (0.9 ps), the maximum population of which is predicted to be less than 20% at any time during electron transfer. Given these facts, together with the signal-to-noise characteristics of our data, it is likely that in our data set any absorbance changes arising from $P^+B_L^-$ will be obscured by the formation and decay of B*.

The SAS corresponding to P* in all of the mutants (Figure 4; solid lines) showed a small but consistent negative feature slightly to the red of the initial bleach of the B band (at approximately 805 nm), which may be contributed to by several processes. Due to poor signal to noise and time resolution a small fraction of either B* or $P^+B_L^-$ may be mixed in to the fitted spectrum, which was assigned to the P* state. However, we expect that these artifacts are very dependent on P* lifetimes. Since we do not observe major variations over a large range of P* lifetimes, 4-36 ps (Figure 4), we believe that this feature is intrinsic of P*. This assumption is supported by triplet−singlet spectra of *Rb. sphaeroides* RC's, which reveal a similar feature with the same shape and position.[43]

In addition to the SAS, the Global analysis also reveals the lifetimes of the individual states in the model and hence the rate of charge separation in the various mutant complexes (Table 2). Comparison of these lifetimes with the single exponential time constants for the decay of P* stimulated emission derived from the single wavelength data (Table 3) shows that both approaches yield very similar P* decay rates.

Rates of Primary Charge Separation in Membrane Bound RC's. In Table 4, we compare our findings on the rate of primary charge separation in membrane-bound mutant RC's with values published by other groups for detergent-solubilized mutant RC's from either *Rb. sphaeroides* or *Rb. capsulatus*. The values we have obtained in the present study are, on the whole, slower than have been reported by others previously, although as is demonstrated by YM210F, where several studies have been made of an individual mutation, there is considerable variation in the reported values for the charge separation rate (Table 4). As discussed above, a large part of this variation may arise from differences in the experimental conditions employed in the measurement of this reaction. Other pertinent factors are the different species studied and the different preparations used (the RC's examined in Finkele et al. (1990),[16] for example, lacked a considerable fraction of the Q_A quinone). Nevertheless, despite the existing variation in reported rates, the slight acceleration of the rate of charge separation induced by removal of the WT. *Rb. sphaeroides* RC from the membrane[23] also seems to pertain to mutated complexes. Experiments are currently under way to test this more directly by purification of mutated RC's from RC-only membranes and from membranes prepared from antenna-containing stains. The comparison of our biexponential decay kinetics with those reported previously (Table 2) failed to demonstrate any systematic difference in the degree of biexponential character between membrane-bound and solubilized RC's (i.e., the relative amplitudes of the slow and fast components).

In our recent comparison of the time-resolved and steady-state optical properties of WT membrane-bound and solubilized RC's,[23] we discussed the acceleration seen in the rate of charge separation on removal of the RC from the membrane (e.g., 3.3 ps, cf. 4.5 ps from global analysis) in terms of a fine tuning of the charge separation rate as the result of small changes in one or more of the parameters that control the rate of electron transfer. The apparent slowing in the overall rate in membrane-bound mutated complexes revealed by the data in Table 4 can be accounted for in similar terms. For example, it is interesting to see that the E_m for P measured for the WT membrane bound RC was slightly greater then for its solubilized version (Table 2). With all other things being equal, a difference in E_m in the membrane-bound complexes would be expected to result in a smaller ΔG and hence a slower rate of charge separation. We use this small difference between the solubilized and membrane-bound RC's only as an example, because, as indicated above, it is unlikely that the E_m for P is the only rate-controlling parameter that is altered in these mutants.

The Nonmonoexponential Character of P* Decay in RC's. The data presented in this paper confirm our earlier observations on the WT complex,[23] that the nonmonoexponential character of P* decay does not arise from the removal of the RC from the membrane. Alternative explanations of the nonmonoexponential decay of P* have included a mechanism in which the slower component arises from thermal repopulation of P* from the charge separated state,[44] mechanisms involving the participation of "parking states" on the inactive branch,[9] and mechanisms that involve two or more distinct conformational states that give rise to different rates of P* decay.

Nonadiabatic electron transfer is described by the Marcus equation, the simple classical form of which is

$$k_{cs} = \frac{2\pi}{\hbar(4\pi\lambda kT)^{1/2}} V^2 \exp\left[\frac{-(\Delta G + \lambda)^2}{4\lambda kT}\right] \qquad (2)$$

In this expression ΔG is the difference in free energy between the reactant (P*) and product (charge separated) state, V is the electronic coupling, $\hbar$ and k are Planck's constant and the Boltzmann constant, respectively, and k_{cs} is the rate of charge separation. The solvent reorganization energy, λ, is the energy required to distort the nuclear configuration of the reactant state into that of the product state. The rate of electron transfer is maximal when $-\Delta G$ and λ are equal, i.e., $-\Delta G + \lambda = 0$. If the relationship between $\ln(k_{cs})$ and ΔG is plotted, then a parabolic curve results (termed a Marcus parabola), the steepness of which is governed by λ. Because of the temperature dependence of k_{cs}, the WT RC is thought to lie close to the top of the parabola where the rate of electron transfer is near to maximal.[42]

The ΔG for primary electron transfer is the energy difference between P* and the charge separated state, either $P^+H_L^-$ or $P^+B_L^-$, depending on the favored model for the reaction. Changes in ΔG induced by mutation will arise either from a change in the energy of P* and/or from changes in the redox potentials of the P/P^+ couple and the H_L/H_L^- or B_L/B_L^- couple. We can conclude from the absorption spectra of the mutated RC's that the difference in free energy between the ground and excited state of P is unchanged in the mutants, and thus any change in ΔG must arise from a change in the energy of the charge separated state. Changes in the E_m for P/P^+ are listed in Table 2. However, the E_m for both H_L/H_L^- and B_L/B_L^- cannot be measured directly. In analyses of the effects of mutation at the M210/L181 positions on the ΔG for charge separation, the simplifying assumption has been made that the measured change in E_m for P/P^+ is a true measure of the change in ΔG.[22]

Alternatively ΔG may be estimated from measurements of recombination luminescence in RC's where forward electron transfer from H_L^- is blocked by depletion or chemical reduction of Q_A.[28,44,45] Charge recombination to P* is dependent on ΔG by the amount of delayed fluorescence from the repopulated P* state, which occurs on a different time scale to the prompt. However, as the ΔG measured by this technique is that for the reaction $P^* \leftarrow P^+H_L^-$, it is not clear whether this is an appropriate measure of the actual change in free energy associated with the initial step in electron transfer, as the repopulation may involved a relaxed state of $P^+H_L^-$.[44] Furthermore, the initial step of charge separation may in fact be $P^* \rightarrow P^+B_L^-$.[10,11,26]

In the recent work of Jia et al. (1993)[22] the multiexponentiality of P* decay was interpreted in terms of an electron transfer reaction in which there was a spread in the ΔG between the reactant (excited) and product (charge separated) states; both the superexchange and sequential models for primary electron transfer were discussed. Such a distribution in ΔG could arise from a distribution in redox potentials for the P/P^+ and H_L/H_L^- redox couples, in the same way that a slight variation in the conformation of the protein gives rise to inhomogeneous broadening of, for example, the Q_y absorbance band of P.[46] A distribution in free energy gaps would give rise to a distribution in rate constants for charge separation. Of course, by the same token a distribution of protein conformational states could also give rise to distributions in other rate-determining parameters (such as V and λ). For simplicity we will first assume that any distribution in rates arises solely from a distribution in ΔG.

Although it is clear from the results of redox titrations on P (Table 1) that the mutations at the M210/L181 positions influence the mean value of ΔG for charge separation, it is less clear whether these mutations affect a distribution in ΔG ($\delta\Delta G$). Recently reported crystallographic data on RC's from YM210F revealed no striking differences in the structure of the protein relative to the WT.[47] Furthermore, the combination of absorbance and FT-Raman measurements on the various M210 mutants suggests no major changes in the environment of the pigments or their interaction.[31] If $\delta\Delta G$ is indeed independent of the identity of the residues at the M210 and L181 positions, then this would result in a distribution in rate constants for charge separation that is rather narrow near the top of the Marcus parabola and which gets broader on each side of the parabola. Jia et al. have used this concept to fit their data on the effects of mutation on the rates of P* decay in detergent-solubilized M210/L181 mutants of *Rb. capsulatus* to a distribution in ΔG.[22] In their analysis they found that all their measurements of the rate of P* decay could be accounted for by assuming that the mean value of ΔG is affected by the mutation, while $\delta\Delta G$ is constant, with a value of approximately 130 cm^{-1}. The exacerbation in the degree of nonmonoexponential character seen in mutants with relatively large increases or decreases in the E_m for P relative to the WT (and hence in ΔG) is explained by the broader distribution in rate constants in the wings of the Marcus parabola (if $\delta\Delta G$ is constant).

Rather than analyze our data by using a distribution in ΔG, and thus make assumptions concerning which of the rate-governing parameters are affected by protein inhomogeneities and by the mutations, we have directly fitted our single wavelength data on P* decay using a Gaussian distribution of rate constants (eq 1). The variable parameters in the fit are the central rate (k), the relative width of the distribution (σ), and

its height. From the Marcus equation, if $\delta\Delta G$ is the only distribution that gives rise to the distribution in rate constants and if $\delta\Delta G$ is constant irrespective of the mean value of ΔG (as proposed by Jia et al.[22]), then the value of σ should increase as ΔG is increased or decreased relative to the value in the WT complex.

The fits made to our experimental data using this simple analysis were almost as good as the biexponential fits (compare columns 5 and 6 of Table 5). The fact that one parameter less is needed for the distributional fit makes it even more attractive. In all cases the spread of the rates was rather broad (σ is of the order 0.5−0.6 log units). The results of the analysis are shown in Table 5. The main finding from our analysis is that there does not appear to be any structural dependence of σ with the change in the ΔG in the mutants relative to the WT (implied from the change in the E_m for P/P^+; Table 1, column 1). Put another way, our data indicate not that the distribution in rate constants is broader at the sides of the Marcus parabola than it is at the top but rather that the distribution is more or less the same regardless of the position on the parabola. This is in contrast to the analysis of Jia et al.[22] described above and suggests either that (1) $\delta\Delta G$ decreases as ΔG increases or decreases relative to that in the WT or that (2) $\delta\Delta G$ is not the main determinant of the nonmonoexponential decay in RC's. The first of these explanations is rather counterintuitive, as it would require perturbation of the system through mutagenesis to be accompanied by less heterogeneity in the protein. Furthermore, hole burning experiments performed on both WT and YM210F[48] did not resolve differences in the vibronic and linewidth parameters of the primary donor. Therefore we feel that the second explanation is the more likely. The conclusion that $\delta\Delta G$ is unlikely to be the main source of the nonmonoexponential kinetics of P* decay was also arrived at by Small and co-workers[46] on the basis of hole burning studies of the WT complex.

As yet, it is not clear why we should arrive at a different conclusion to that reported by Jia et al. (1993).[22] We are currently investigating the kinetics of P* decay in detergent solubilized mutant RC's isolated from *Rb. sphaeroides* RC-only strains and from antenna-containing strains in order to investigate this point further.

In addition to $\delta\Delta G$, small variations in the structure of the RC protein could also give rise to a distribution in V, which depends upon the edge-to-edge distance between the donor and acceptor molecules and their relative orientations.[42] A distribution in electronic couplings (δV) would also give rise to a distribution in rates but, in contrast to a distribution in ΔG, the distribution in rates arising from δV would be independent of the value of ΔG. We observe that the width of the distribution in $\ln(k_{cs})$ is independent of the charge separation rate.

As can be seen from eq 2, $\ln(k_{cs})$ is linear in $2^* \ln(V)$ ($=\ln(V^2)$) and thus in $\ln(\delta V)$. If a distribution in V would be the main contributor to the rate distribution, then $\ln(\delta V)$ is expected to be independent of the charge separation rate. The electronic coupling can be described by $V = V_o \exp(-\beta R)$, with β and V_o constant. Since $\ln(k) \sim \ln(V)$ and $\ln(V) \sim R$, we can state that a distribution in $\ln(k_{cs})$ may be directly related to a distribution in R. Thus the observation of a distribution which does not vary with the charge separation rate would infer that the distribution in R, δR, is not influenced by the mutation.

Finally, we turn to the question of a possible distribution in λ in the WT, and whether it is possible that the magnitude of λ is altered by mutation at the M210/L181 positions. From the Marcus equation it can be seen that the reorganization energy has a complex influence on the rate of electron transfer. λ is likely to be sensitive to changes in, and small fluctuations of, the structure of the protein around and between the pigments involved in the electron transfer reaction. In addition, λ is expected to rise with increasing polarity of the environment of the redox centers involved in charge separation and hence might be expected to be sensitive to the chemical identity of the residue at the M210 position. Unfortunately, λ is a parameter which may not be assessed through direct experiment, and so we have no evidence that RC's exhibit a distribution in λ. However, it has been suggested recently, on the basis of the observed response of the absorption band of B_L, that the ability of the protein to undergo relaxation in response to the reduction of H_L is altered upon mutagenesis of the M210 residue, the degree of this alteration appearing to correlate with the extent of modulation of the rate of electron transfer.[49] This alteration has been interpreted in terms of a change in the reorganization energy in the mutated RC's.

The Effects of Reducing Q_A on Primary Charge Separation. In accord with our recent findings on the WT complex[23] we have observed that prereduction of Q_A leads to a slowing of the rate primary electron transfer in the M210 mutants. The decrease in the rate of electron transfer was most marked in the mutant RC's which had the slowest rates of electron transfer (YM210L and YM210W). The most straightforward explanation for the effect of Q_A reduction is that the negative charge on the quinone creates an electric field which influences the rate at which the electron is transferred from P to B_L/H_L. The result of a charge on Q_A can be modeled by calculating its effect on the energy levels of the charge separated states, $P^+B_L^-$ or $P^+H_L^-$, and thus the energy gap ΔG. Up to this point we have not discussed the possibility of fitting a Marcus parabola (eq 2) to the charge separation rates as a function of the redox potential of P,[21,22] where the latter is considered to be a measure of ΔG. If we do so we obtain a value for the reorganization energy λ of about 400 cm^{-1}. Now assuming that reduction of Q_A only decreases the energy gap, ΔG, and leaves the other parameters unchanged, we can estimate a mean value for the change in ΔG by placing the charge separation rates measured for Q_A reduced RC's on the same parabola but at lower values for ΔG. We find an average decrease of ΔG of approximately 240 cm^{-1} as a result of the reduction of Q_A.

We can further estimate the effect of a negative charge on Q_A on the energy gap by calculating the Coulombic interaction of the charge on Q_A on the redox potentials of the other pigments, using the distances from the crystal structure. The value calculated in this way should be of the same order of magnitude as the estimated value given above. This is only possible, using a reasonable value for ϵ_r, if we assume that the initial charge separation process is $P^* \rightarrow P^+B_L^-$. In that case a value for ϵ_r of 3.5 results in a calculated energy difference of 250 cm^{-1}. To obtain a similar change in the value for the energy gap of the $P^* \rightarrow P^+H_L^-$, as a result of the reduction of Q_A, an unrealistically large value for ϵ_r of 12 is required.

The classical electron transfer model explains the dependence of the charge separation rate on ΔG reasonably well, both in the case of changes in the redox potential of P and in the case of prereduction of Q_A. However, as discussed above, to explain the multiexponential decay of P* we cannot use a distribution in ΔG. This is in contrast with measurements on isolated RC's[22,50,51] and on PSII RC's and RC−core complexes,[52] in which nonexponential kinetics could be analyzed in terms of a distribution in ΔG. Within the framework of classical electron transfer, we may be able to explain the results in terms of a distribution in V. As we have pointed out, this could arise from a variability in the distance between the cofactors. Although

we have strong indications that this may be the case,[26] further experiments should support this.

On the other hand, there are also measurements which clearly show that dynamics occur on the time scale of electron transfer. Recent results in the region of 1000−1600 cm^{-1} have shown a very fast (∼200 fs) relaxation process upon excitation of P.[53] Furthermore, on a picosecond time scale wavelength dependences of the P* decay have been interpreted in terms either of relaxation of P* [28] or of a wavelength dependent charge separation rate.[26,54] Peloquin et al.[44] have proposed a relaxation of $P^+H_L^-$ based on time correlated single photon timing measurements. This model may also explain the discrepancy between measurements of ΔG using different techniques involving different time scales.[28,44]

The relaxation processes are expected to be a consequence of protein dynamics on time-scales ranging from subpicosecond through to milliseconds. Eventually this may result in a time dependent conformational adjustment of the protein to excitation and moving charges and may lead to a model in which the radical pairs, $P^+B_L^-$ and $P^+H_L^-$, relax in time.[44] Usually it is very hard to distinguish between a static distribution in ΔG or a relaxation resulting in an increase of ΔG with time; however, with these experiments we have shown that a static distribution cannot explain the multiexponential decay of P* in the frame of classical electron transfer theory.

Conclusions

Our results are not consistent with a distribution of charge separation rates that arises solely from a distribution in free energies. Furthermore, it seems unlikely that the modulation of the overall rate of electron transfer seen in the M210 mutants arises solely from the measured shift in the midpoint potential for the P/P^+ redox couple, as there is also indirect evidence that shifts in the midpoint potential for the H_L/H_L^- couple contribute to a change in the driving force for charge separation in at least some of the mutants that we have examined. To our knowledge there is no evidence that excludes the possibility that V and/or λ are changed as a consequence of mutation at the M210 position, and certainly the second of these parameters is known to be sensitive to the polarity of the medium surrounding the redox centers that participate in the electron transfer reaction. On the basis of a two step model for charge separation, the slowing of the rate of P* decay seen in the membrane-bound mutant RC's is consistent with the predicted effect of a negative charge on Q_A on the free energy change between P* and $P^+B_L^-$. However, if electron transfer from P* to H_L is a one step reaction, then it seems unlikely that quinone reduction modulates the rate of P* decay solely through a change in ΔG for the reaction.

Acknowledgment. R.V., L.B. and R.V.G. acknowledge support from the Dutch Foundation for Life Sciences. P.M.G. acknowledges financial support from the Wellcome Trust. M.R.J. is a BBSRC Senior Research Fellow. This work was supported by EC Contracts CT92-0796 and CT93-0278. We thank Frank van Mourik; without his help this work would not have been possible.

References and Notes

(1) Deisenhofer, J.; Michel, H.; Huber, R. *TIBS* **1982**, 243.

(2) Deisenhofer, J.; Epp, O.; Miki, K.; Huber, R.; Michel, H. *Nature* **1985**, *318*, 618.

(3) Allen, J. P.; Feher, G.; Yeates, T. O.; Komiya, H.; Rees, K. C. *Proc. Natl. Acad. Sci. U.S.A.* **1987**, *84*, 5730.

(4) El-Kabbani, O.; Chang, C.-H.; Tiede, D.; Norris, J.; Schiffer, M. *Biochemistry* **1991**, *30*, 5361.

(5) Ermel, U.; Michel, H.; Schiffer, M. *J. Bioenerg. Biomembr.* **1994**, *26*, 5.

(6) Feher, G.; Allen, J. P.; Okamura, M. Y.; Rees, D. C. *Nature* **1989**, *339*, 111.

(7) Martin, J. L.; Breton, J.; Hoff, A. J.; Migus, A.; Antonetti, A. *Proc. Natl. Acad. Sci. U.S.A.* **1986**, *83*, 957. Kirmaier, C.; Holten, D. *Proc. Natl. Acad. Sci. U.S.A.* **1990**, *87*, 3552. Fleming, G. R.; Martin, J. L.; Breton, J. *Nature* **1988**, *333*, 190.

(8) Nagarajan, V.; Parson, W. W.; Gaul, D.; Schenck, C. *Proc. Natl. Acad. Sci. U.S.A.* **1990**, *87*, 7888.

(9) Hamm, P.; Gray, K. A.; Oesterhelt, D.; Feick, R.; Scheer, H.; Zinth, W. *Biochim. Biophys. Acta* **1993**, *1142*, 99.

(10) Holzapfel, W.; Finkele, U.; Kaiser, W.; Oesterhelt, D.; Scheer, H.; Stilz, H. U.; Zinth, W. *Chem. Phys. Lett.* **1989**, *160*, p 1.

(11) Holzapfel, W.; Finkele, U.; Kaiser, W.; Oesterhelt, D.; Scheer, H.; Stilz, H. U.; Zinth, W. *Proc. Natl. Acad. Sci. U.S.A.* **1990**, *87*, 8168.

(12) Arlt, T.; Schmidt, S.; Kaiser, W.; Lauterwasser, C.; Meyer, M.; Scheer, H.; Zinth, W. *Proc. Natl. Acad. Sci. U.S.A.* **1993**, *90*, 11757.

(13) Bixon, M.; Jortner, J.; Michel-Beyerle, M. E.; Ogrodnik, A. *Biochim. Biophys. Acta* **1989**, *977*, 273.

(14) Bixon, M.; Jortner, J. *J. Phys. Chem.* **1991**, *95*, 1941.

(15) Chan, C.-K.; Chen, L. X.-Q.; DiMagno, T. J.; Hanson, D. K.; Nance, S. L.; Schiffer, M.; Norris, J. R.; Fleming, G. R. *Chem. Phys. Lett.* **1991**, *176*, 366.

(16) Finkele, U.; Lauterwasser, C.; Zinth, W.; Gray, K. A.; Oesterhelt, D. *Biochemistry* **1990**, *29*, 8517.

(17) Yeates, T. O.; Komiya, H.; Chirino, A.; Rees, D. C.; Allen, J. P.; Feher, G. *Proc. Natl. Acad. Sci. U.S.A.* **1988**, *85*, 7993.

(18) Parson, W. W.; Chu, Z.-T.; Warshel, A. *Biochim. Biophys. Acta* **1990**, *1012*, 251.

(19) Muller, M. G.; Griebenow, K.; Holzwarth, A. R. *Chem. Phys. Lett.* **1993**, *199*, 465.

(20) Du, M.; Rosenthal, S. J.; Xie, X.; DiMagno, T. J.; Schmidt, M.; Hanson, D. K.; Schiffer, M.; Norris, J. R.; Fleming, G. R. *Proc. Natl. Acad. Sci. U.S.A.* **1992**, *89*, 8517.

(21) DiMagno, T. J.; Rosenthal, S. J.; Xie, X.; Du, M.; Chan, C. K.; Hanson, D.; Schiffer, M.; Norris, J. R.; Fleming, G. R. In *The Photosynthetic Bacterial Reaction Center II*; Breton, J., Vermeglio, A.; Eds.; Plenum Press: New York, 1992; p 209.

(22) Jia, Y.; DiMagno, T. J.; Chan, C.-K.; Wang, Z.; Du, M.; Hanson, D. K.; Schiffer, M.; Norris, J. R.; Fleming, G. R.; Popov, M. S. *J. Phys. Chem.* **1993**, *97*, 13180.

(23) Beekman, L. M. P.; Visschers, R. W.; Monshouwer, R.; Heer-Dawson, M.; Mattioli, T. A.; McGlynn, P.; Hunter, C. N.; Robert, B.; van Stokkum, I. H. M.; van Grondelle, R.; Jones, M. R. *Biochemistry* **1995**, *34*, 14712.

(24) Dressler, K.; Umlauf, E.; Schidt, S.; Hamm, P.; Zinth, W.; Buchanan, S.; Michel, H. *Chem. Phys. Lett.* **1991**, *183*, 270.

(25) Schmidt, S.; Arlt, T.; Hamm, P.; Lauterwasser, C.; Finkele, U.; Drews, G.; Zinth, W. *Biochim. Biophys. Acta* **1993**, *1144*, 385.

(26) Beekman, L. M. P.; Jones, M. R.; von Stokkum, I. H. M.; van Grondelle, R. In *Research in Photosynthesis*; Matis, P., Ed.; Kluwer Academic Publishers: Dordrecht, 1995.

(27) Jones, M. R.; Fowler, G. J. S.; Gibson, L. C. D.; Grief, G. G.; Olsen, J. D.; Crielaard, W.; Hunter, C. N. *Mol. Microbiol.* **1992**, *6*, 1173−1884. Jones, M. R.; Visschers, R. W.; van Grondelle, R.; Hunter, C. N. *Biochemistry* **1992**, *31*, 4458.

(28) Nagarajan, V.; Parson, W. W.; Davis, D.; Schenck, C. C. *Biochemistry* **1993**, *32*, 12324.

(29) Shochat, S.; Arlt, T.; Francke, C.; Gast, P.; van Noort, P. I.; Otte, S. C. M.; Schelvis, H. P. M.; Schmidt, S.; Vijgenboom, E.; Vrieze, J.; Zinth, W.; Hoff, A. J. *Photosynth. Res.* **1994**, *40*, 55.

(30) Marcus, R. A.; Sutin, M. *Biochim. Biophys. Acta* **1985**, *811*, 265.

(31) Jones, M. R.; Heer-Dawson, M.; Mattioli, T. A.; Hunter, C. N.; Robert, B. *FEBS Lett.* **1994**, *399*, 18.

(32) Visser, H. M.; Somsen, O. J. G.; van Mourik, F.; Lin, S.; van Stokkum, I. H. M.; van Grondelle, R. *Biophys. J.* **1995**, *69*, 1083.

(33) van Stokkum, I. H. M.; Brouwer, A. M.; van Ramesdonk, H. J.; Scherer, T. *Proc. Kon. Akad. Wetensch.* **1993**, *96*, 43. Van Stokkum, I. H. M.; Scherer, T.; Brouwer, A. M.; Verhoeven, J. W. *J. Phys. Chem.* **1994**, *98*, 852.

(34) Kwa, S. L. S.; Volker, S.; Tilly, N. T.; van Grondelle, R.; Dekker, J. P. *Photochem. Photobiol.* **1994**, *59*, 219.

(35) Gray, K. A.; Farchaus, J. W.; Wachtveitl, J.; Breton, J.; Oesterhelt, D. *EMBO J.* **1990**, *9*, 2061.

(36) Beekman, L. M. P.; van Mourik, F.; Jones, M. R.; Visser, H. M.; Hunter, C. N.; van Grondelle, R. *Biochemistry* **1994**, *33*, 3143.

(37) Schiffer, M.; Chan, C.-K.; Chang, C.-H.; DiMagno, T. J.; Fleming, G. R.; Nance, S.; Norris, J.; Snyder, S.; Thurnauer, M.; Tiede, D. M.; Hanson, D. K. In *The Photosynthetic Bacterial Reaction Center II*; Breton, J., Verméglio, A., Eds.; **1992**, 351−361, Plenum Press: New York; 1992; pp 351−361.

(38) Breton, J. *Biochim. Biophys. Acta* **1985**, *810*, 234.

(39) Breton, J. In *The Photosynthetic Bacterial Reaction Center II*; Breton, J., Vermeglio, A., Eds.; Plenum Press: London; NATO ASI Series, 1988.

(40) Steffen, M.; Lao, K. Q.; Boxer, S. G. *Science* **1994**, *264*, 810.

(41) Murchison, H. A.; Alden, R. G.; Allen, J. P.; Peloquin, J. M.; Taguchi, A. K. W.; Woodbury, N. W.; Williams, J. C. *Biochemistry* **1993**, *32*, 3498.

(42) Moser, C. C.; Keske, J. M.; Warncke, K.; Farid, R. S.; Dutton, P. L. *Nature*, **1993**, *355*, 796.

(43) Lous, E. J.; Hoff, A. J. In *The Photosynthetic Bacterial Reaction Center I*; Breton, J., Vermeglio, A., Eds.; Plenum Press: London; NATO ASI Series, 1988.

(44) Peloquin, J. M.; Williams, J. C.; Lin, X.; Alden, R. G.; Taguchi, A. K. W.; Allen, J. P.; Woodbury, N. W. *Biochemistry* **1994**, *33*, 8089.

(45) Woodbury, N. W.; Parson, W. W. *Biochim. Biophys. Acta* **1984**, *767*, 345.

(46) Small, G. J.; Hayes, J. M.; Silbey, R. J. *J. Phys. Chem.* **1992**, *96*, 7499.

(47) Chirino, A. J.; Lous, E. J.; Huber, M.; Allen, J. P.; Schenck, C. C.; Paddock, M. L.; Feher, G.; Rees, D. C. *Biochemistry* **1994**, *33*, 4584.

(48) Middendorf, T. R.; Mazzola, L. T.; Gaul, D. F.; Schenck, C. C.; Boxer, S. G. *J. Phys. Chem.* **1991**, *95*, 10142.

(49) Spiedel, D.; Heer-Dawson, M.; Mattioli, T. A.; Hunter, C. N.; Jones, M. R.; Robert, B., unpublished data.

(50) Ogrodnik, A.; Nenpp, W.; Volk, M.; Aumeier, G.; Michel-Beyerle, M. E. *J. Phys. Chem.* **1994**, *98*, 3432.

(51) Bixon, M.; Jortner, J.; Michel-Beyerle, M. E. *Chem. Phys.* **1995**, *197*, 389.

(52) Groot, M. L.; Peterman, E. J. G.; van Kan, P. J. M.; van Stokkum, I. H. M.; Dekker, J. P.; van Grondelle, R. *Biophys. J.* **1994**, *67*, 318.

(53) Hamm, P.; Zinth, W. *J. Phys. Chem.* **1995**, *99*, 13537.

(54) Vos, M. H.; Jones, M. R.; Hunter, C. N.; Breton, J.; Martin, J.-L. *Proc. Natl. Acad. Sci. U.S.A.* **1994**, *92*, 12701.

JP953054H